ELSEVIER

Journal of Nuclear Materials 290–293 (2001) 1112–1116

journal of nuclear materials

www.elsevier.nl/locate/jnucmat

Experimental study of radiation power flux on the target surface during high heat plasma irradiation

V.N. Litunovsky *, I.B. Ovchinnikov, V.A. Titov

D.V. Efremov Scientific Research Institute of Electrophysical Apparatus, Science Technical Center Sinteza, Sovetsky pr.1, 189631 St. Petersburg, Russian Federation

Abstract

Some new data of the experimental study of visible radiation from the plasma shielding layer (SL) on the target surface during high heat plasma–material interaction are given in the report. The experiments were performed on the VIKA facility. Long pulse ($\tau_p = 0.36$ ms) high power ($P_{irr} \sim 100$ GW m^{-2} plasma streams were used for irradiation of graphite and tungsten samples. The target inclination ($\alpha = 0°$ normal irradiation; 45°; 70°) and magnetic field ($B = 0$ to 3 T) were varied in experiments. It is shown that the values of ($\Delta\lambda \approx 400$ to 700 nm) visible radiation power flux (VRPF) on the target surface can be characterised by the level of $P_R \sim 1$ GW m^{-2} for normal irradiation in the presence of a magnetic field $B = 2$ to 3 T. Inclination of targets leads to the reduction of this flux in conformity with the corresponding decrease of the irradiation power. The material of the target does not influence sufficiently on the level of the incident radiation power flux in the performed experiments. © 2001 Published by Elsevier Science B.V.

Keywords: High heat plasma irradiation; Plasma disruption; Shielding layer; Radiation flux

1. Introduction

One of the critical items in the problem of understanding and prediction of material erosion under high heat plasma load relevant to plasma disruptions in ITER is to determine the level of the power flux which reaches the divertor target surface taking into account the shielding effect of the material plasma layer generated above the target surface from ionised erosion products. Both numerical modelling and experimental simulation have asked for help to decide this problem (see for example [1,2]).

As a first step to solve the problem to determine incident power flux, the level of power flux absorbed by irradiated sample was measured. It is shown that the measured values can be characterised by the level of absorbed power $P_{abs} \sim 3$ to 5 GW m^{-2} for different materials (Al, W, graphite) irradiated by a plasma power flux $P_{irr} \sim 100$ GW m^{-2} [3]. It is supposed that this level is close to the average level of power flux on the target surface from the shielding layer (SL). First experimental data about the visible radiation from SL on the target surface are given in [4,5].

This paper describes the results of direct measurements of the visible radiation power flux (VRPF) on the target surface at high power plasma loading with a level and duration which are expected during plasma disruptions in ITER. Such data are interesting for numerical codes verification and practical applications too (plasma treatment of structural materials, etc.).

2. Experimental conditions

A long-pulse coaxial plasma accelerator is the source of plasma high heat flux in the VIKA facility [6]. The sectionalised power supply – pulse forming network (5 kV, 100 kJ) – allows one to form rectangular current pulses in the plasma gun that results in quasi-stationary plasma parameters during the pulse duration. The level of impurities in hydrogen plasma does not exceed ~1%

* Corresponding author. Tel.: +7-812 462 7991; fax: +7-812 464 4623.

E-mail address: vlitun@niiefa.spb.su (V.N. Litunovsky).

0022-3115/01/$ - see front matter © 2001 Published by Elsevier Science B.V.
PII: S0022-3115(00)00666-8

for any mode of operation. The ion energy is $\varepsilon_i \sim 200$ eV. The effective diameter of the plasma stream is $d_p \sim 0.04$ m.

A variation of both the specific plasma heat flux ($w_p \leqslant 30$ MJ m^{-2}) and the pulse duration ($\tau_p = 0.09$ to 0.36 ms) is possible. In all described experiments the mode with a pulse duration $\tau_p = 0.36$ ms was used.

The quasi-stationary magnetic field was produced by two coils in the interaction chamber and was varied in the range $B = 0$ to 3 T. To understand possible effects of the target inclination (damp target plates in tokamak divertor) both a field normal to the target surface ($\alpha = 0°$) and inclined ($\alpha = 45°$; 70°) was used.

Samples of graphite (EK-98) and tungsten were used in the described experiments. The square of the samples overlapped the cross-section of the plasma stream, the thickness was $h = 10^{-2}$ m.

To study the parameters of the incident visible radiation an optical scheme with a quartz fiber (length $L = 6$ m; diameter $d = 10^{-3}$ m) inserted into the inclined hole in the target body was used. The light collected by the fiber was guided to an analysing setup (spectrograph or monochromator) and registered (film or photomultiplier).

To measure the absolute amount of the radiation power flux a calibration of the optical tract with certificated tungsten lamp was performed. Typically the detected wavelength range was limited to $\Delta\lambda \approx 400$ to 700 nm.

3. Experimental results

As a first step the registration of the observation SL plasma spectra for graphite and tungsten targets in visible spectral range was undertaken. The fragments of two typical spectra for graphite target are shown in Fig. 1.

The presence of carbon spectral lines CII, CIII and CIV, the most intensive being the lines CII ($z = 1$), is typical for such spectra. The spectra are characterised also by the presence of some impurities (Al, Mn, Na, Ca, Cu, Si) and hydrogen spectral lines. The most probable source of the most impurities is the plasma gun, and the quartz fiber (specially for Si). The continuum radiation gives the most contribution to the detected radiation. The spectrum is characterised also by a growth of the continuum intensity in the long-wave region of spectrum.

One can see that the application of the magnetic field results in a ~2–3 fold growth of the continuum radiation intensity. The main reason of this is most probably the growth of the SL plasma density (see the evolution of the half-width of H_β line with the growth of the magnetic field on the fragments of tungsten target spectra in Fig. 2). The electron density (data of H_β line broadening measurements) increases from $n_e \sim 10^{22}$ m^{-3} in the absence of magnetic field up to $n_e \geqslant 10^{24}$ m^{-3} in the presence of a 3 T magnetic field. The estimation of the electron temperature (from carbon lines intensities correlation) of the radiating plasma gives the values (in different exposures) of $T_e \cong 1$ to 3 eV.

A typical oscillogram of the detected radiation intensity is shown in Fig. 3. The time delay of the sharp growth of the radiation intensity of 30–50 μs corresponds to the real front of irradiation power. The detailed temporal behaviour of the radiation intensity depends on the registered wavelength and irradiation conditions in general. But one can mark the typical feature of most of the signals: the intensity falls off in the

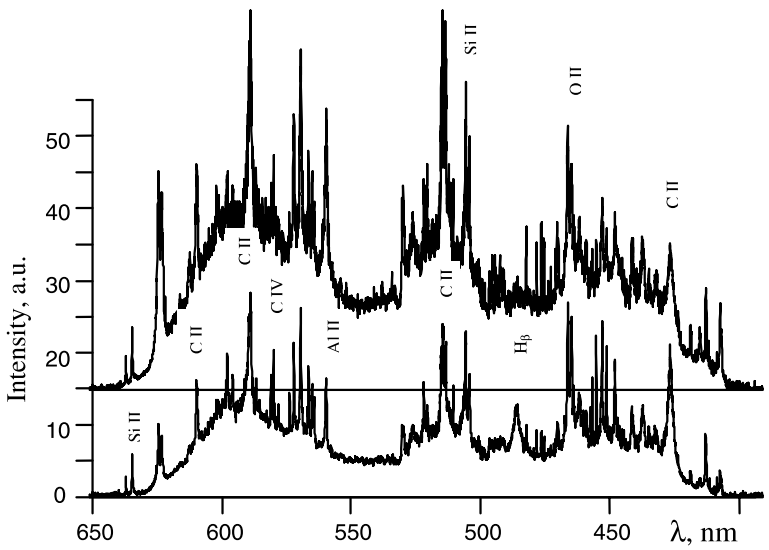

Fig. 1. Fragments of the typical spectra for the visible radiation in front of the target surface without (bottom) and with (top) 2.5 T normal magnetic field. Target – graphite. Irradiation power is $P_{irr} \sim 100$ GW m^{-2}.

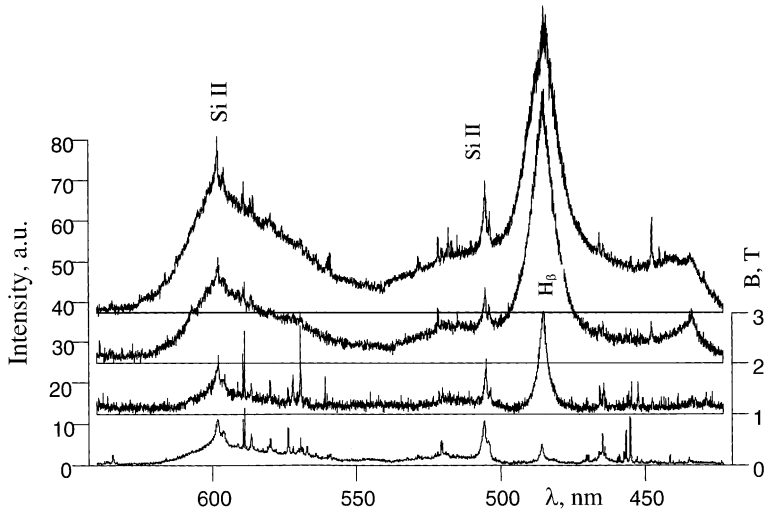

Fig. 2. Fragments of typical spectra of visible radiation in a neighbourhood of H_β line for different values of normal magnetic field. Target – tungsten. Irradiation power is $P_{irr} \sim 100$ GW m^{-2}.

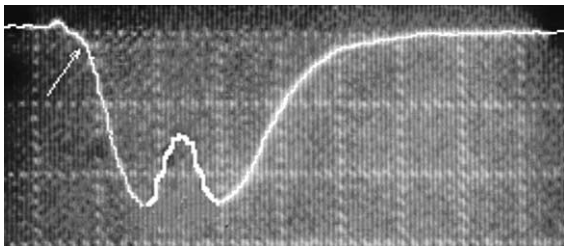

Fig. 3. Typical oscillogramm of detected radiation ($\lambda =$ 670 nm) intensity. $B = 3$ T. $P_{irr} = 120$ GW m^{-2}. The time scale is 0.1 ms/div. The pointer shows the start of irradiation. $P_{irr} =$ 120 GW m^{-2}.

middle of pulse. The correlation of the peak amplitudes, the duration and depth of fall are varied depending of the irradiation conditions. A decreasing irradiation power due to the variation of the plasma gun voltage or target inclination results in a decrease of the amplitude of the first sub-pulse. Besides the delay time of sharp growth of its intensity is increased.

Direct measurements of VRPF on tungsten and graphite targets surface were performed with variation of the magnetic field, the sample inclination and the irradiation power for each material. For convenience all received data are presented separately by dependencies for each varied parameter.

The growth of the relative radiation intensity shown in the spectroscopic data with the magnetic field is confirmed by the measurements of the absolute values of VRPF too. As shown in Fig. 4, there is the saturation of the measured values level of around $P_R \sim 1$ GW m^{-2} for magnetic field $B \geqslant 2$ T.

The evolution of average values of VRPF on graphite and tungsten samples due to the variation of

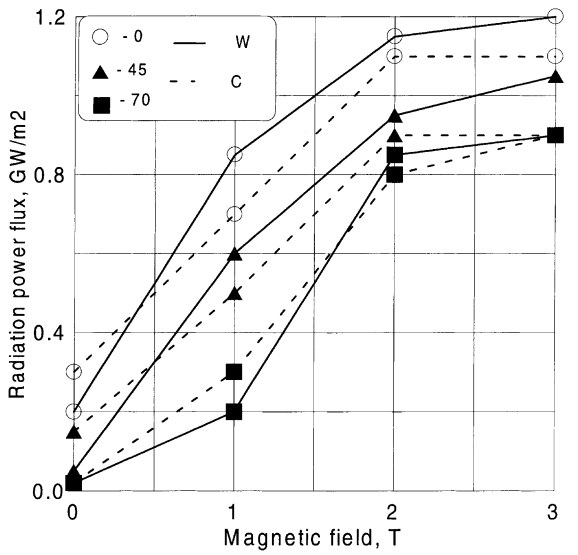

Fig. 4. Visible radiation power flux on the target surface versus magnetic field at different inclination of target (circle: normal irradiation; triangle: $\alpha = 45°$; square: $\alpha = 70°$). $P_{irr} =$ 120 GW m^{-2}.

the target inclination at different values of magnetic field is shown in Fig. 5. The inclination of the target leads naturally to a decrease of the incident radiation flux. To understand the nature of this effect measurements of the radiation power flux with variation of the irradiation power during PFN voltage variation (at normal irradiation) was performed. The comparison of these data with those obtained by the variation of the irradiation power during sample inclination shows reasonably good agreement (Fig. 6). So, one can believe that the main

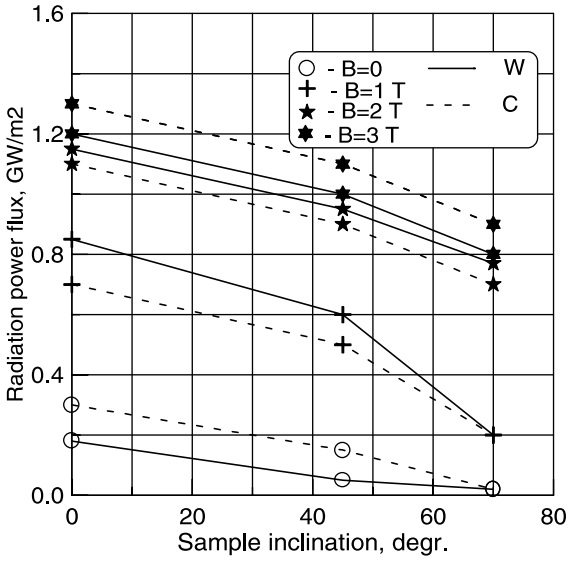

Fig. 5. Visible radiation power flux on the target surface versus sample inclination at different values of the magnetic field.

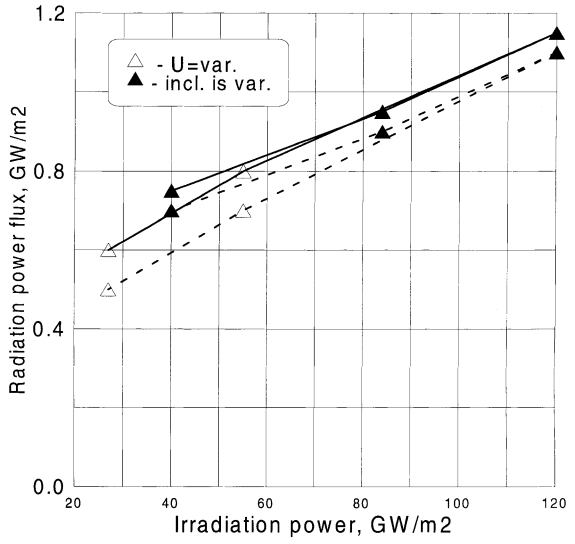

Fig. 6. Radiation power flux on the target surface versus irradiation power flux varied by plasma gun voltage and sample inclination. The white triangles give data for marked values of irradiation power (normal irradiation). Black triangles – data for inclination 0°, 45° (calculated $P_{irr} = 84$ GW m^{-2}) and 70° ($P_{irr} = 40$ GW m^{-2}).

cause of observed decrease of the VRPF with sample inclination is the corresponding decrease of the irradiation power.

The above a level of $P_R \sim 1$ GW m^{-2} is achieved in general in the second half of the irradiation pulse with decreased power flux $P_{irr} \leqslant 50$ GW m^{-2}.

In spite of strong difference in the characteristics of the irradiated materials a clear influence on the level of the measured VRPF is not seen.

4. Discussion and conclusions

For the first time direct measurements of the radiation power flux on a target surface have been performed. They allow one to get new knowledge on the power flux which reaches the target surface during high heat plasma loading.

The observed spectra in visible region are rather different from those obtained by a one at side-on observation performed earlier [7]. The most probable cause of this is the strong absorption of the visible radiation in a dense SL plasma ($n_e \cong 3 \times 10^{24}$ m^{-3}).

The most probable cause for the growth of the incident radiation flux by applying of the magnetic field ($B = 2$ to 3 T) is the growth of plasma density in the SL due to suppression of SL lateral plasma losses.

The observed decrease of the radiation intensity (and hence probably the total incident power flux) in the middle of the irradiation pulse is the most probable cause of pause in erosion observed before by us [3]. In turn the probable reason of such a decrease is the increasing opacity of the SL due to plasma density growth. The opacity of the SL plasma for visible radiation was experimentally observed earlier in our experiments too [7].

Assuming a Plank distribution of the spectral intensity of the total radiation from the SL plasma, the total radiation power flux on the target reaches a level of around few GW m^{-2} at the emitted plasma temperature of $T_e \sim 1$ eV. This is in a satisfactory agreement with measured level of absorbed power of $P_{abs} \sim 3$ to 4 GW m^{-2} which can include in general the radiation and the heat conduction power fluxes. In this case it means that the radiation power flux determines to a considerable extent the level of the total power flux which reaches the target surface during the high heat plasma loading.

No surprising effects have been seen in the behaviour of the incident power flux by inclination of the target: the radiation power flux decreases accordingly to the decrease of the irradiation power due to inclination of the target.

In spite of strong difference in the type of the irradiated materials the level of VRPF on the target surface is practically not changed. It is in a good agreement with our previous measurements of the power flux absorbed by the target during irradiation [3]. As to possible explanation of this fact one can suppose on the base of modern notion that only lowest plasma layer of SL is responsible mainly for observed radiation flux. Such a most dense layer which is close to the target surface has the lowest temperature. The last one depends feebly on target material. Besides such a layer is optically thick

and is able to protect effectively target against more short wave radiation from upper layers of more hot (but less dense) plasma. Naturally the composition of plasma (type of material) determines the spectral distribution of radiation intensity from upper layers [8].

Application of the magnetic field suppresses the lateral losses of plasma from the SL due to the improvement of radial plasma confinement and results in the growth of the radiation intensity.

The received data do not contradict the results of our previous experimental study of high power plasma–material interaction and can be used for verification of numerical codes and evaluation of expected power flux on the divertor target surface during off-normal events in existing and future fusion machines. Such data are also useful for the choice of the plasma irradiation mode in plasma technology (pulse plasma treatment of the structural materials).

Acknowledgements

The authors are grateful to Dr V. Kuznetsov for technical assistance. The work is performed under partial support of ISTC (Project #539).

References

[1] N. Arkhipov, V. Bakhtin, B. Bazylev, I. Landman, V. Safronov, D. Toporkov, S. Vasenin, H. Wuerz, A. Zhitlukhin, Fus. Tecchnol. 32 (1997) 45.
[2] H. Wuerz, B. Bazylev, F. Kappler, I. Landman, G. Piazza, S. Peschni, J. Nucl. Mater. 233–237 (1996) 798.
[3] V.N. Litunovsky, V.E. Kuznetsov, I.B. Ovchinnikov, V.A. Titov, in: Proceedings of the 20th Symposium on Fusion Technology, Fus. Technol. 1 (1998) 59.
[4] V.N. Litunovsky, V.E. Kuznetsov, B.V. Lyublin, I.B. Ovchinnikov, V.A. Titov, A. Hassanein, Material response due to simulated plasma disruption loads, Presented at ISFNT-5 Rome, 19–24 September 1999.
[5] V.N. Litunovsky, I.B. Ovchinnikov, V.A. Titov, in: 10th International Toki Conference on Plasma Physics and Controlled Nuclear Fusion, Physics and Technology for Steady State Plasmas, Toki, Japan, 18–21 January 2000.
[6] V.M. Kozhevin, V.N. Litunovsky, B.V. Lyublin, I.B. Ovchinnikov, V.A. Titov, A.A. Drozdov, V.E. Kuznetsov, Fus. Eng. Des. 28 (1995) 157.
[7] V.N. Litunovsky, I.B. Ovchinnikov, V.A. Titov, B.V. Lyublin, J. Plasma Fus. Res. Ser. 2 (1999) 324.
[8] N. Arkhipov, V. Bakhtin, S. Kurkin, V. Safronov, D. Toporkov, S. Vasenin, H. Wuerz, A. Zhitlukhin, J. Nucl. Mater. 233–237 (1996) 767.